Design and Performance of Kilo-Pixel TES Arrays for ACTPol

E. A. Grace, J. A. Beall, J. Britton, H. M. Cho, M. J. Devlin, A. E. Fox, G. C. Hilton, J. Hubmayr, K. D. Irwin, J. Klein, M. Lungu, L. B. Newburgh, J. P. Nibarger, M. D. Niemack, J. McMahon, L. A. Page, C. Pappas, B. L. Schmitt, S. T. Staggs, and E. J. Wollack

***Abstract*—ACTPol, a polarization sensitive receiver for the Atacama Cosmology Telescope, is designed to make sensitive maps of the cosmic microwave background anisotropies at arcminute scales and millimeter wavelengths by employing three arrays of superconducting transition edge sensor (TES) detectors. The ACTPol TES bolometers have a target superconducting transition temperature of 150 mK and will be cooled to a bath temperature of 100 mK with a dilution refrigerator enabling increased array sensitivity. Each array will consist of ∼1000 TES detectors coupled to a micromachined silicon feedhorn stack via superconducting ortho-mode transducers and transmission lines. The superconducting detectors of the first ACTPol array have been characterized in their final receiver configuration with measurements of key TES parameters including the transition temperature, saturation power, and thermal conductance.**

***Index Terms*—Bolometer, cosmic microwave background (CMB), polarimetry, transition edge sensor (TES).**

I. Introduction

THE cosmic microwave background (CMB) has proven to be a powerful probe of cosmology through observations of its intrinsic and secondary temperature anisotropies. Polarization sensitive measurements of the CMB will enable even further insights into the history and structure of the universe. Measurements of this signal at small angular scales promise to constrain properties of dark energy and the sum of the neutrino masses, measure the primordial helium abundance, and improve constraints on the spectral index of inflation n_s [1], [2].

The polarization signal of the CMB is significantly fainter than the temperature signal placing stringent requirements on the instrument sensitivity required for such a measurement. Current technology achieves nearly background limited noise response in individual detectors. Thus, increasing the sensitivity of next generation instruments requires large focal planes containing arrays of many detectors. ACTPol, a polarization sensitive upgrade to the Atacama Cosmology Telescope (ACT), will explore these fundamental physics questions using observations of the temperature and polarization anisotropies of the CMB at arcminute scales using such arrays [3]. ACT is a dual-reflector telescope located in the Atacama Desert in Chile consisting of an off axis Gregorian configuration with a 6-meter primary mirror [4], [5].

The new ACTPol receiver targets three large arrays of polarization sensitive detectors: two arrays with 150 GHz sensitivity and one multichroic array with simultaneous 90 GHz and 150 GHz sensitivity. These detector arrays will operate based on superconducting transition edge sensor (TES) technology [6]. Each of the three arrays will be housed in a separate optics tube comprised of three cryogenic silicon lenses and band defining filters. The detectors will be cooled to an operating temperature of 100 mK using a pulse tube backed dilution refrigerator. Through this combination of telescope resolution and increased instrument sensitivity, ACTPol will explore the fundamental physics questions described above.

II. Detector and Wafer Design

The ACTPol pixel design consists of a planar orthomode transducer (OMT) and two transition edge sensors as seen in Fig. 1. The planar detector chip is coupled to a dual mode waveguide input and a quarterwave delay with a backshort termination [7]. On the detector chip a pair of opposing antennas are used to couple each polarization [8]. From the OMT the signal is directed onto niobium microstrip lines through a coplanar waveguide to microstrip transition. The radiation is then carried onto its corresponding TES island where the power is deposited as heat through long meanders of lossy gold microstrip. This heats the TES island, which has a weak thermal link (G) to the bath temperature through its four silicon nitride legs [9]. The change in temperature is then detected by the TES itself, which is fabricated from a molybdenum-copper bilayer tuned to have a transition temperature (T_c) of around 150 mK. The full pixel design as well as the structure of an individual TES can be seen in Fig. 1.

Manuscript received October 9, 2012; accepted January 18, 2012. Date of publication January 22, 2013; date of current version February 27, 2013. This work was supported by the U.S. National Science Foundation through awards AST-0965625, PHY-0855887, and PHY-1214379. The NIST authors would like to acknowledge the support of the NIST Quantum Initiative. The works of E. A. Grace and B. Schmitt were supported by the NASA Office of the Chief Technologists Space Technology Research Fellowship awards.

E. A. Grace, L. B. Newburgh, L. A. Page, C. Pappas, and S. T. Staggs are with Joseph Henry Laboratories of Physics, Jadwin Hall, Princeton University, Princeton, NJ 08544 USA.

J. A. Beall, J. Britton, H. M. Cho, A. E. Fox, G. C. Hilton, J. Hubmayr, K. D. Irwin, J. P. Nibarger, and M. D. Niemack are with NIST Quantum Devices Group, Boulder, CO 80305 USA.

M. J. Devlin, J. Klein, M. Lungu, and B. L. Schmitt are with the Department of Physics and Astronomy, University of Pennsylvania, Philadelphia, PA 19104 USA.

J. McMahon is with the Physics Department, University of Michigan, Ann Arbor, MI 48109 USA.

E. J. Wollack is with NASA/Goddard Space Flight Center, Greenbelt, MD 20771 USA.

Color versions of one or more of the figures in this paper are available online at http://ieeexplore.ieee.org.

Digital Object Identifier 10.1109/TASC.2013.2242191

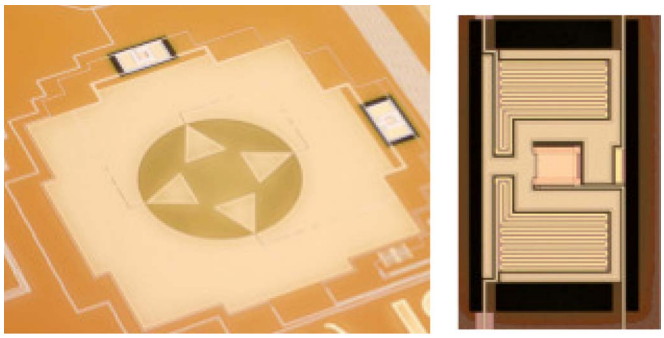

Fig. 1. (Left) Full ACTPol pixel. The four triangular probes in the center of the pixel comprise the OMT, which couples to the incoming radiation with orthogonal pairs of probes coupling to the two components of the polarization. This power is then carried to one of the TES islands via the niobium microstrip lines. (Right) Individual TES. The TES is isolated from the bath temperature by four silicon nitride legs which carry the TES input and bias lines. The power carried onto the island from the OMT is deposited via the lossy gold microstrip.

These pixels are fabricated on monolithic three-inch wafers at NIST in Boulder, CO. The ACTPol science wafers come in two varieties, the hex wafer and the semihex wafer. The hex wafer contains 127 pixels (254 TESes) while the semihex wafer contains 47 pixels (94 TESes). In total, one full ACTPol 150 GHz array contains 522 pixels and 1044 TESes. The readout of the full array uses a three-stage SQUID time domain multiplexing (TDM) scheme [10], [11] in which groups of between 64 and 94 detectors are biased on the same bias line. This places stringent uniformity requirements on the wafer properties in order to achieve optimal sensitivity on all simultaneously biased detectors.

In total, there were twelve potential science wafers fabricated for the first ACTPol array. From these twelve the six final deployment wafers were selected - three hex wafers (W10, W09, and W02) and three semihex wafers (SH1A, SH2A, SH2B). A fourth hex wafer (W08) which was not tested in the ACTPol cryostat with these wafers but had excellent performance in separate dark and optical tests will replace W02 in the final array configuration.

III. Wafer Parameter Characterization

The wafer selection process was conducted through initial dark characterization of each of the twelve potential ACTPol science wafers in a dilution-refrigerator-based test-bed at Princeton University designed for this purpose. The six wafers selected for the first ACTPol array were chosen from this characterization based on the criteria of detector yield, detector parameter accuracy, and wafer uniformity. These six wafers were then assembled into their final configuration in the ACTPol cryostat where characterization of the detector electrothermal and optical properties was conducted.

There are a number of key TES parameters which determine the successful operation of the detector and must therefore be carefully tuned in the fabrication process. Among the most important such parameters are the transition temperature (T_c), the saturation power at which the detector is driven normal (P_{sat}), and the thermal conductivity to the bath temperature (G). The target values of these three key parameters for the ACTPol detector pixels are $T_c = 150$ mK, $P_{sat} = 13.5$ pW, and $G = 240$ pW/K.

TABLE I
Measured Average ACTPol Detector Parameter Values and Detector Yield by Wafer for the First 150 GHz Array

Wafer	Yield (%)	T_c (mK)	P_{sat} (pW)	G (pW/K)
W10	71	142 ± 5	8.6 ± 1.9	231 ± 29
W09	69	141 ± 6	8.4 ± 1.7	226 ± 29
W02	71	154 ± 6	12.7 ± 3.9	308 ± 56
SH1A	73	155 ± 5	14.3 ± 1.7	338 ± 31
SH2A	80	156 ± 6	14.4 ± 2.0	342 ± 35
SH2B	78	151 ± 3	11.8 ± 2.7	310 ± 18
Overall	72	148 ± 8	10.7 ± 3.5	259 ± 59

The transition temperatures of the detectors were measured by raising the temperature of the cold stage of the ACTPol cryostat in 5 mK steps through the range of expected transition temperatures. After observing the steps between which the detector moved from its superconducting state to its normal state, the T_c was taken to be the average of these two temperatures.

The saturation power of the detectors (P_{sat}) has been defined for these measurements as the power needed to bias the detectors at 50% of the normal resistance value (R_n) at the operational bath temperature. The target value for the saturation power was selected to be three times the expected optical loading conditions in the field (predicted to be approximately 4 pW with variation due to the water vapor content of the atmosphere and the optical efficiency of the detectors). This value was measured for each detector by driving the TES normal and then ramping the bias value down through the transition and finding the point at which the resistance value was 50% of R_n.

The resulting measurement of the average transition temperature for the full array was $T_c = 148 \pm 8$ mK and for the saturation power was $P_{sat} = 10.7 \pm 3.5$ pW. These results are satisfactory for measurements in the field. The majority of the variation in these parameters arises due to differences between different wafers. The measured wafer level uniformity per wafer in T_c is such that variations are at or below the 5% level. The wafer level uniformity in P_{sat} (excluding wafer W02 which has an unusual amount of variation) shows variations at or below the 20% level. After W02 is replaced by W08 all array wafers will have variation in P_{sat} at or below the 20% level.

Another important property of the detectors is the thermal conductivity of the connection between the island and the bath (G). This was determined by first measuring the saturation power at a range of bath temperatures and then fitting the relation in (1) for κ and n. Then, G can then be found by taking the derivative of this expression with respect to the temperature at $\mathrm{T} = T_c$ as shown in (2):

$$P(T) = \kappa \left(T^n - T_b^n\right) \tag{1}$$

$$G = \frac{dP}{dT}(T_c) = n\kappa T_c^{n-1}. \tag{2}$$

The overall average results of the fit for κ and n were $\kappa = 6850 \pm 2500$ pW/K^n and $n = 3.3 \pm 0.25$. The resulting average and standard deviation of the thermal conductivity is $G = 272 \pm 59$ pW/K.

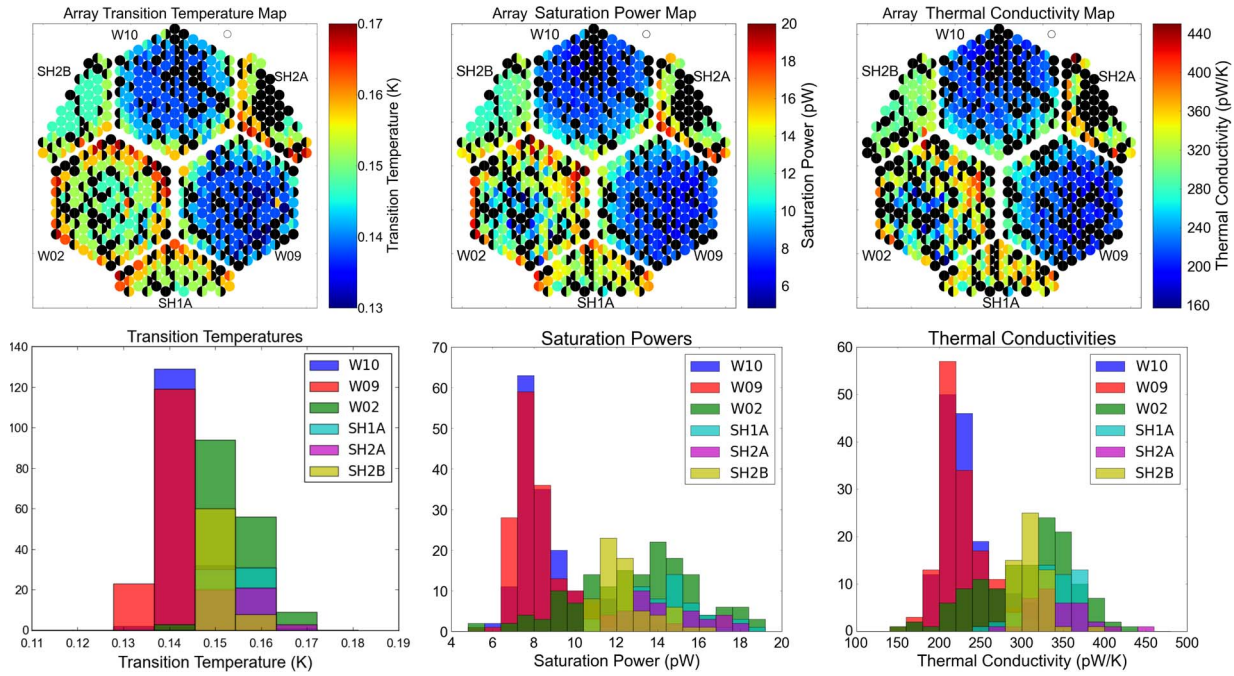

Fig. 2. Distributions of the measured detector parameters across the array. From left to right are the detector transition temperatures, saturation powers, and thermal conductances. Each pixel is represented by a circle with the value for each TES is displayed as half that circle. It can be seen that the largest variations in parameter value occur between the wafers while the wafer level uniformity is quite high. The wafers W09 and W10 can be seen to have the highest level of uniformity. Wafer W02 is less uniform and will be replaced for the final configuration as described in the text.

In addition to maintaining excellent uniformity and accuracy of the wafer parameter values, ensuring high detector yield on these large wafers is a priority. The detector yield of the full array was characterized in the ACTPol cryostat setup where detector failures originate either on the wafer itself or from opens or shorts in the readout circuitry. The overall measured yield of the first 150 GHz array was 72%. However, a large portion of the reduced yield is known to originate from correctable problems in the readout circuitry. Prior to deployment these issues will be corrected allowing for a predicted overall yield of 81%.

A summary of the average wafer parameter measurements as well as the yield results can be seen in Table I. The measured distributions of these parameters can be seen in Fig. 2.

IV. Conclusion

These measurements have demonstrated the achievement of sufficient detector uniformity on the wafer level with the large W9 and W10 hex wafers showing only 5-20% variation in transition temperature, saturation power, and thermal conductivity. Understanding the effect of fabrication process changes on the differences in parameter values among wafers will remain a priority in the fabrication of wafers for the future ACTPol arrays.

Acknowledgment

The authors would like to thank B. Harrop for the work in the bonding and assembly of the first array.

References

[1] K. M. Smith, A. Cooray, S. Das, S. Doré, D. Hanson, C. Hirata, M. Kaplinghat, B. Keating, B. LoVerde, N. Miller, G. Rocha, M. Shimon, and O. Zahn, "CMBPol mission concept study: Gravitational lensing," 2008, arxiv:0811.3916.

[2] K. Ichikawa, T. Sekiguchi, and T. Takahashi, "Primordial helium abundance from CMB: A constraint from recent observations and a forecast," *Phys. Rev. D, Part. Fields*, vol. 78, no. 4, pp. 043509-1–043509-10, Aug. 2008.

[3] M. D. Niemack, P. A. R. Ade, J. Aguirre, F. Barrientos, J. A. Beall, J. R. Bond, J. Britton, H. M. Cho, S. Das, M. J. Devlin, S. Dicker, J. Dunkley, R. Dünner, J. W. Fowler, A. Hajian, M. Halpern, M. Hasselfield, G. C. Hilton, M. Hilton, J. Hubmayr, J. P. Hughes, L. Infante, K. D. Irwin, N. Jarosik, J. Klein, A. Kosowsky, T. A. Marriage, J. McMahon, F. Menanteau, K. Moodley, J. P. Nibarger, M. R. Nolta, L. A. Page, B. Partridge, E. D. Reese, J. Sievers, D. N. Spergel, S. T. Staggs, R. Thornton, C. Tucker, E. Wollack, and K. W. Yoon, "ACTPol: A polarization- sensitive receiver for the Atacama Cosmology Telescope," in *Proc. SPIE Astron. Telesc. Instrum.*, 2010, vol. 7741, pp. 774 11S-1–774 11S-21.

[4] J. W. Fowler, M. D. Niemack, S. R. Dicker, A. M. Aboobaker, P. A. R. Ade, E. S. Battistelli, M. J. Devlin, R. P. Fisher, M. Halpern, P. C. Hargrave, A. D. Hincks, M. Kaul, J. Klein, J. M. Lau, M. Limon, T. A. Marriage, P. D. Mauskopf, L. Page, S. T. Staggs, D. S. Swetz, E. R. Switzer, R. J. Thornton, and C. E. Tucker, "Optical design of the atacama cosmology telescope and the millimeter bolometric array camera," *Appl. Opt.*, vol. 46, no. 17, pp. 3444–3454, Jun. 2007.

[5] D. S. Swetz, P. A. R. Ade, M. Amiri, J. W. Appel, E. S. Battistelli, B. Burger, J. Chervenak, M. J. Devlin, S. R. Dicker, W. B. Doriese, R. Dunner, T. Essinger-Hileman, R. P. Fisher, J. W. Fowler, M. Halpern, M. Hasselfield, G. C. Hilton, A. D. Hincks, K. D. Irwin, N. Jarosik, M. Kaul, J. Klein, J. M. Lau, M. Limon, T. A. Marriage, D. Marsden, K. Martocci, P. Mauskopf, H. Moseley, C. B. Netterfield, M. D. Niemack, M. R. Nolta, L. A. Page, L. Parker, S. T. Staggs, O. Stryzak, E. R. Switzer, R. Thornton, C. Tucker, E. Wollack, and Y. Zhao, "The atacama cosmology telescope: The receiver and instrumentation," NASA, Hanover, MD, USA, 2010, arXiv:1007.0290.

[6] K. D. Irwin and G. C. Hilton, "Transition edge sensors," in *Cryogenic Particle Detection*, C. Enss, Ed. Berlin, Germany: Springer-Verlag, 2005.

[7] E. J. Wollack, "Photolithographic orthomode transducers," *J. Phys., Conf. Ser.*, vol. 155, no. 012006, pp. 42–50, 2009.

[8] J. J. McMahon, J. W. Appel, J. E. Austermann, J. A. Beall, D. Becker, B. A. Benson, L. E. Bleem, J. Britton, C. L. Chang, J. E. Carlstrom, H. M. Cho, A. T. Crites, T. Essinger-Hileman, W. Everett, N. W. Halverson, J. W. Henning, G. C. Hilton, K. D. Irwin, J. Mehl, S. S. Meyer, S. Mossley, M. D. Niemack, L. P. Parker, S. M. Simon, S. T. Staggs, C. Visnjic, E. Wollack, K. U-Yen, K. W. Yoon, and Y. Zhao, "Planar orthomode transducers for feedhorn-coupled TES polarimeters," in *Proc. 13th Int. Workshop LTD*, 2009, vol. 1185, pp. 490–493.

[9] K. Y. Yoon, J. W. Appel, J. E. Austermann, J. A. Beall, D. Becker, B. A. Benson, L. E. Bleem, J. Britton, C. L. Chang, J. E. Carlstrom, H.-M. Cho, A. T. Crites, T. Essinger-Hileman, W. Everett, N. W. Halverson, J. W. Henning, G. C. Hilton, K. D. Irwin, J. McMahon, J. Mehl, S. S. Meyer, S. Moseley, M. D. Niemack, L. P. Parker, S. M. Simon, S. T. Staggs, K. U-Yen, C. Visnjic, E. Wollack, and Y. Zhao, "Feedhorn-coupled TES polarimeters for next-generation CMB instruments," in *Proc. 13th Int. Workshop LTD–AIP Conf.*, 2009, vol. 1185, pp. 515–518.

[10] P. A. J. De Korto, J. Beyer, S. Deiker, G. C. Hilton, K. D. Irwin, M. Macintosh, S. W. Nam, C. D. Reintsema, L. R. Vale, and M. E. Huber, "Time-division superconducting quantum interference device multi- plexer for transition-edge sensors," *Rev. Sci. Instrum.*, vol. 74, no. 8, pp. 3807–3815, Aug. 2003.

[11] E. S. Battistelli, M. Amiri, B. Burger, M. Halpern, S. Knotek, M. Ellis, X. Gao, D. Kelly, M. Macintosh, K. Irwin, and C. Reintsema, "Functional description of read-out electronics for time-domain multi-plexed bolometers for millimeter and sub-millimeter astronomy," *J. Low Temp. Phys.*, vol. 151, no. 3/4, pp. 908–914, May 2008.